



This is a repository copy of *Enhancing Autonomy in VTOL Aircraft Based on Symbolic Computation Algorithms*.

White Rose Research Online URL for this paper:
<http://eprints.whiterose.ac.uk/99730/>

Version: Accepted Version

Proceedings Paper:

Douthwaite, J.A., Mihaylova, L.S. and Veres, S.M. (2016) Enhancing Autonomy in VTOL Aircraft Based on Symbolic Computation Algorithms. In: Towards Autonomous Robotic Systems. 17th Annual Conference of Towards Autonomous Robotic Systems, June 26--July 1, 2016, Sheffield, UK. Lecture Notes in Computer Science, 9716 . Springer International Publishing . ISBN 978-3-319-40378-6

https://doi.org/10.1007/978-3-319-40379-3_10

Reuse

Unless indicated otherwise, fulltext items are protected by copyright with all rights reserved. The copyright exception in section 29 of the Copyright, Designs and Patents Act 1988 allows the making of a single copy solely for the purpose of non-commercial research or private study within the limits of fair dealing. The publisher or other rights-holder may allow further reproduction and re-use of this version - refer to the White Rose Research Online record for this item. Where records identify the publisher as the copyright holder, users can verify any specific terms of use on the publisher's website.

Takedown

If you consider content in White Rose Research Online to be in breach of UK law, please notify us by emailing eprints@whiterose.ac.uk including the URL of the record and the reason for the withdrawal request.



eprints@whiterose.ac.uk
<https://eprints.whiterose.ac.uk/>

Enhancing Autonomy in VTOL Aircraft Based on Symbolic Computation Algorithms

James A. Douthwaite, Lyudmila S. Mihaylova, Sandor M. Veres

Dept. of Automatic Control Systems Engineering,
University of Sheffield, United Kingdom
jadouthwaite1@sheffield.ac.uk, l.s.mihaylova@sheffield.ac.uk,
s.veres@sheffield.ac.uk

Abstract. Research into the autonomy of small Unmanned Aerial Vehicles (UAVs), and especially on Vertical Take Off and Landing (VTOL) systems has intensified significantly in recent years. This paper develops a generic model of a VTOL UAV in symbolic form. The novelty of this work stems from the designed Model Predictive Control (MPC) algorithm based on this symbolic model. The MPC algorithm is compared with a state-of-the-art Linear Quadratic Regulator algorithm in attitude rate acquisition and its more accurate performance and robustness to noise is demonstrated. Results for the controllers designed for each of the aircraft's angular rates are presented in response to input disturbances.

1 Introduction

Vertical Take-off and Landing (VTOL) aircraft are unique in having a propulsion system that allows the generation of lift independently of the aircraft's velocity. This affords the vehicle to conduct controlled manoeuvres in scenarios where other vehicles may be unable to operate. More recently, the growth of micro-Unmanned Aerial Vehicle (UAV) technology has seen a rise in interest in developing compact VTOL systems as a platform for a range of applications, such as search and rescue, ordinance surveying and aerial cinematography [2]. The current applications of these systems are however, limited by the level of autonomy that has been achieved to allow the system to handle events that could otherwise compromise the vehicle. Robust control regimes able to handle events such as gusts, or rotor loss are highly desirable in enhancing the future of autonomous vehicles.

One of the most powerful methods for control is the Model Predictive Control (MPC) [14]. Recent advances for MPC algorithms are presented in the recent survey [10]. Although widely applied to industrial systems, partially to fixed-wing aircraft and UAV formations [4], the MPC application to VTOL is still limited. One of the main advantages of the MPC is that it can provide both the desired level of performance and safety. This is especially important for small VTOL aircraft, who's applications may be limited by their resilience to disturbances. Efficient numerical methods for non-linear MPC and moving horizon estimation

are presented in [5]. Other efficient algorithms for linear small scale control are presented in [9]. Although a significant efforts have been devoted to both linear and non-linear MPC, including in [12] its application to VTOL UAVs is still limited.

Hence, in this paper we explore the advantages on the MPC approach in the light of VTOL craft. The MPC performance is compared with a Linear Quadratic Gaussian (LQG) regulator and its accuracy is demonstrated.

The main contributions of this paper stem from: i) the developed symbolic model of the VTOL UAV. The model is general and comprises all possible motions and changes in 3D manoeuvres. ii) the designed MPC algorithm to conduct attitude changes taking into account the design constraints of the VTOL aircraft. As a VTOL we consider the quadrotor UAV shown on Figure 1.

The rest of the paper is as follows. The second section a symbolic approach to modelling a generic VTOL aircraft is proposed. In the third section, the flight dynamics of a quadrotor micro-UAV are introduced; which uses two rotor pairs to generate a body thrust and torque vector. The fourth section then outlines the design of the two control regimes; a Model Predictive Controller (MPC) and Linear Quadratic Regulator (LQR) for angular rate acquisition. Section five evaluates the performance of the two controllers through discussion and comparison. Finally, conclusive remarks on the effectiveness of the controllers are provided, and the implications each controller's use are discuss in conclusion.



Fig. 1: F450 quadrotor layout and 3D CAD assembly.

2 Rigid Body Analysis and Modelling

The aircraft is free to move in all six Degrees of Freedom (DOF) with linear and angular velocities; $\mathbf{v}_1 = [u, v, w]^T$ and $\omega_{CG} = \mathbf{v}_2 = [p, q, r]^T$, respectively. The aircraft's body can be approximated as a point mass (m) with a symbolic inertia

matrix (\mathbf{I}_{CG}). Forces due to the atmosphere and gravitation act on the airframe in the global axes, these require that they be translated into the body frame of axes before they can be introduced into the model:

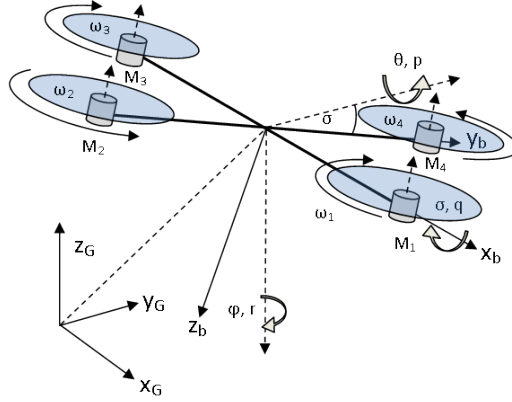


Fig. 2: The Earth and body reference axes.

Using standard aerospace convention, the body frame rotation can be described in Earth coordinates in Euler angles (as shown in Figure 2). The rotational arguments can be combined to form the directional co-sine matrix *DCM* [3],[6],[7]:

$$\mathbf{DCM}_{GB} = \begin{bmatrix} c(\theta)c(\psi) & c(\theta)s(\psi) & -s(\theta) \\ s(\phi)s(\theta)c(\psi) - c(\phi)s(\psi) & c(\phi)c(\psi) + s(\phi)s(\theta)s(\psi) & s(\phi)c(\theta) \\ s(\phi)s(\psi) + c(\phi)s(\theta)c(\psi) & c(\phi)s(\theta)s(\psi) - s(\phi)c(\psi) & c(\phi)c(\theta) \end{bmatrix}, \quad (1)$$

where $c(\theta)$ and $s(\theta)$ denotes the *cos* and *sin* functions, respectively. This allows gravity and other external forces to be mapped onto the body axis reference frame, as shown in equations (1) and (2) [8],[13]

$$\mathbf{f}_g = m\mathbf{g} = \mathbf{DCM}_{GB} * \begin{bmatrix} 0 \\ 0 \\ mg \end{bmatrix}. \quad (2)$$

The resultant force acting on the aircraft, currently neglecting the VTOL propulsion system, is in the form:

$$m\dot{\mathbf{v}}_1 = \mathbf{f} - (\mathbf{v}_2 \times \mathbf{v}_1). \quad (3)$$

Here the resultant linear acceleration can be seen as the difference between the body momentum and the external force vector, \mathbf{f} . Similarly, the sources of

torque are modelled by the vector, τ , which acts to induce an instantaneous change in angular momentum $\dot{\mathbf{h}}$ [7],[8]:

$$\dot{\mathbf{h}} = \mathbf{I}_b \dot{\mathbf{v}}_2 = \tau - (\dot{\mathbf{v}}_2 \times \mathbf{h}). \quad (4)$$

The resultant angular momentum (\mathbf{h}) of the body is that of all the rotary elements of the system. VTOL aircraft typically operate using fans or rotors. These can be represented by an inertial matrix (\mathbf{I}_r) and a rate of rotation (Ω_i):

$$\mathbf{h} = \mathbf{I}_b \mathbf{v}_2 + \mathbf{I}_r (\Omega_1 + \Omega_2 + \dots + \Omega_{4,N}). \quad (5)$$

The above matrix expressions can be written in the combined form (6)-(7). This allows the aircraft's body kinematics to be represented as a series of matrix coefficients [8]:

$$\begin{bmatrix} \mathbf{f} \\ \tau \end{bmatrix} = \mathbf{M} \dot{\mathbf{v}} + \mathbf{N} \mathbf{v} + \mathbf{C} \quad (6)$$

or

$$\begin{bmatrix} \mathbf{f} \\ \tau \end{bmatrix} = \begin{bmatrix} m\mathbf{I}_{3 \times 3}, & \mathbf{0}_{3 \times 3} \\ \mathbf{0}_{3 \times 3}, & \mathbf{I}_{CG} \end{bmatrix} \begin{bmatrix} \dot{\mathbf{v}}_1 \\ \dot{\mathbf{v}}_2 \end{bmatrix} + \begin{bmatrix} mS(\mathbf{v}_2), & \mathbf{0}_{3 \times 3} \\ \mathbf{0}_{3 \times 3}, & -S(\mathbf{h}_{CG}) \end{bmatrix} \begin{bmatrix} \mathbf{v}_1 \\ \mathbf{v}_2 \end{bmatrix} + \begin{bmatrix} \mathbf{0}_{3 \times 3}, & \mathbf{R} \\ \mathbf{0}_{3 \times 3}, & \mathbf{0}_{3 \times 3} \end{bmatrix}. \quad (7)$$

Here the function S is used to map the enclosed vector to the matrix space, where \mathbf{R} represents the constant gravitational force acting on the vehicle. Other forces and torques acting on the body, such as control inputs can be seen as an additional term (\mathbf{C}) which must also be converted into the body acceleration vector. The above expression can also be divided through by the inertial matrix to define the systems 6DOF acceleration vector. The final non-linear system is then seen in equation (8):

$$\begin{bmatrix} \dot{\mathbf{v}}_1 \\ \dot{\mathbf{v}}_2 \end{bmatrix} = \left(\begin{bmatrix} mS(\mathbf{v}_2), & \mathbf{0}_{3 \times 3} \\ \mathbf{0}_{3 \times 3}, & -S(\mathbf{h}_{CG}) \end{bmatrix} \begin{bmatrix} \mathbf{v}_1 \\ \mathbf{v}_2 \end{bmatrix} + \begin{bmatrix} \mathbf{0}_{3 \times 3}, & \mathbf{R} \\ \mathbf{0}_{3 \times 3}, & \mathbf{0}_{3 \times 3} \end{bmatrix} + \mathbf{C} \right) \begin{bmatrix} m\mathbf{I}_{3 \times 3} & \mathbf{0}_{3 \times 3} \\ \mathbf{0}_{3 \times 3} & \mathbf{I}_{CG} \end{bmatrix}^{-1}. \quad (8)$$

The VTOL aircraft's full non-linear equations of motion have derived symbolically. In this paper, the dynamics associated with a small quadrotor micro-UAV are now introduced to allow a control mechanism to be designed. In addition to the dynamics, several assumptions were introduced to simplify the resulting model [2]. We assume that the aircrafts body axis are parallel with the Euler axis of rotation, therefore the following relationships are true:

$$\dot{p} = \ddot{\phi}, p = \dot{\phi}, \dot{q} = \ddot{\theta}, q = \dot{\theta}, \dot{r} = \ddot{\psi}, r = \dot{\psi}. \quad (9)$$

Similarly, for the linear states:

$$\dot{u} = \ddot{x}, u = \dot{x}, \dot{v} = \ddot{y}, v = \dot{y}, \dot{w} = \ddot{z}, w = \dot{z}. \quad (10)$$

The aircraft was assumed to be symmetrical in two dimensions, reducing the inertia of the system to a diagonal matrix. The rotors are completely symmetrical and identical, with negligible blade flapping. The resulting thrust vector is also parallel to the quadrotor body z-axis.

3 Quadrotor Dynamics

So far, a generalised rigid body problem has been proposed. Using the Matlab toolbox for symbolic computation, the full 6 Degree of Freedom (DOF) system definition was derived. A quadrotor was chosen to example the characteristics of a VTOL micro-UAV. The quadrotor's propulsion mechanism consists of four groups of propellers, Brushless Motors and Electronic Speed Controllers (ESC). In this instance, each group generates a thrust that acts parallel to the vertical body axis vector at distance l from the center of mass (11).

Using blade element theory, the total body axis thrust generated by the rotor can be approximated symbolically [2],[15]:

$$f_T = C_T \rho A (\Omega R)^2 = k_T \cdot \Omega^2 \quad (11)$$

where C_T is the thrust coefficient, k_T is a constant described in detail below. Here ρ is the air density, A is cross-sectional area of the rotor of radius R . Similarly, the net hub force (H), can be written proportional to the rotor angular velocity (equation (12))[2]. The hub force constant (k_H) is then expressed as:

$$f_H = C_H \rho A (\Omega R)^2 = k_H \cdot \Omega^2. \quad (12)$$

The quadrotor's control matrix is then defined in equation

$$\mathbf{u} = \begin{bmatrix} U_1 \\ U_2 \\ U_3 \\ U_4 \end{bmatrix} = \begin{bmatrix} L \\ M \\ N \\ T_z \end{bmatrix} = \begin{bmatrix} 0 & -k_T |\bar{l}_2| & 0 & k_T |\bar{l}_4| \\ k_T |\bar{l}_1| & 0 & -k_T |\bar{l}_3| & 0 \\ -k_H |\bar{l}_1| & k_H |\bar{l}_2| & -k_H |\bar{l}_3| & k_H |\bar{l}_4| \\ k_T & k_T & k_T & k_T \end{bmatrix} \begin{bmatrix} \Omega_1^2 \\ \Omega_2^2 \\ \Omega_3^2 \\ \Omega_4^2 \end{bmatrix}. \quad (13)$$

This describes how the propulsion system acts to induce corrective body axis forces and torques. Inverting this matrix also provide the necessary mapping for the control mechanism to command a given body axis torque. In addition to the static thrust properties, the propulsion groups each have an associated rise-time (T_S) to achieve a set-point angular velocity (Ω_i). This relationship was found experimentally to be of first order (see Figure 3), with area of proportionality sufficient to allow the approximation of k_T and k_H :

$$R(s) = \frac{k_T}{1 + T_s s} = \frac{0.0529}{1 + 0.108s}. \quad (14)$$

This expression then describes the relationship between set point and instantaneous angular velocity of the rotor. The dynamics of other VTOL aircraft can be approximated similarly, however these expressions were sufficient to represent the dynamics of the quadrotor.

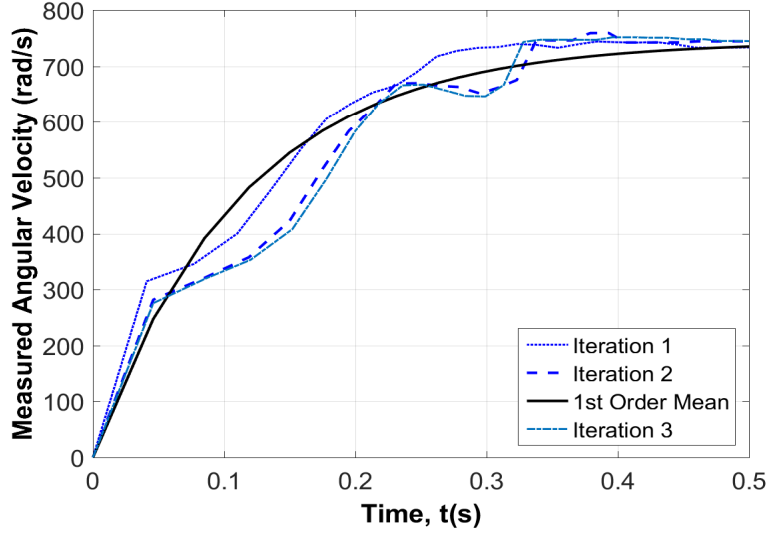


Fig. 3: Approximation of the rotor transient response to a set input at its maximum rotational velocity.

4 Control Design

This approximation allows the representation of the aircraft's states in terms of the body axis coordinate system and Euler rotations. The complete symbolic non-linear model can then be represented by the following expressions:

$$\frac{d\mathbf{x}}{dt} = \begin{bmatrix} \ddot{x} \\ \ddot{y} \\ \ddot{z} \\ \ddot{\psi} \\ \ddot{\theta} \\ \ddot{\phi} \end{bmatrix} = \begin{bmatrix} \dot{\theta}\dot{z} - \dot{\psi}\dot{y} - g\sin(\theta) \\ \dot{\psi}\dot{x} - \dot{\phi}\dot{z} + g\cos(\theta)\sin(\phi) \\ \dot{\phi}\dot{y} - \dot{\theta}\dot{x} + g\cos(\phi)\cos(\theta) - (\Omega_1 + \Omega_2 + \Omega_3 + \Omega_4)k_t/m \\ (I_{33}^b - I_{22}^b)\dot{\theta}\dot{\psi}/I_{11}^b + (I_{33}^r\Omega_T\dot{\theta})/I_{11}^b + (\Omega_4 - \Omega_2)k_t l/I_{11}^b \\ (I_{11}^b - I_{33}^b)\dot{\phi}\dot{\psi}/I_{22}^b - (I_{33}^r\Omega_T\dot{\phi})/I_{22}^b + (\Omega_1 - \Omega_3)k_t l/I_{22}^b \\ (I_{22}^b - I_{11}^b)\dot{\phi}\dot{\theta}/I_{33}^b + (-\Omega_1 + \Omega_2 - \Omega_3 + \Omega_4)k_h l/I_{33}^b \end{bmatrix}, \quad (15)$$

where I_{11}^b , I_{22}^b and I_{33}^b are respectively the moments of inertia around the three axes of rotation.

To allow the application of linear control theory, a symbolic application of small perturbation theory is applied directly to equation (15). This technique assumes that the system is operating around a nominal state (\mathbf{x}_0) with small perturbations (\mathbf{x}_d). The completion of a symbolic linearisation allows parameters to be selected to represent different stages of operation. This paper focuses on the design of a linear stability controller operating around the hover state.

The resulting linear system is then of the form:

$$\frac{d\mathbf{x}}{dt} = \mathbf{A}\mathbf{x} + \mathbf{B}\mathbf{u} + \mathbf{w} \quad (16)$$

$$\mathbf{y} = \mathbf{C}\mathbf{x} + \mathbf{D}\mathbf{u} \quad (17)$$

where $\mathbf{x} = [x, y, z, \psi, \theta, \phi, \dot{x}, \dot{y}, \dot{z}, \dot{\psi}, \dot{\theta}, \dot{\phi}]^T$ is the state vector, \mathbf{A} is the state transition matrix, \mathbf{B} is the control matrix, the control vector containing the rotor angular velocities is defined $\mathbf{u} = [\Omega_1^2, \Omega_2^2, \Omega_3^2, \Omega_4^2]^T$. A source of system noise is also added, \mathbf{w} , with a predefined standard deviation of 0.2. The system output vector \mathbf{y} can then be given by equation (17), as a function of state and the output matrices \mathbf{C} and \mathbf{D} .

Direct substitution of the F450 quadrotor design parameters and considering an attitude hold scenario allowed a numeric state-space representation to be obtained. This linear approximation then provides the basis necessary to design linear controller mechanisms to introduce stability around the straight and level condition.

4.1 Model Predictive Control

A second Model Predictive Controller (MPC) was devised as a comparative controller for tracking the error in the aircraft's attitudes. The linearised system model is used directly in the prediction of the future system state across a defined discrete horizon H_N [14]:

The predicted output of the system and control deflections are defined by \mathbf{G} and \mathbf{F} , respectively:

$$\mathbf{F} = \begin{bmatrix} \mathbf{A} \\ \mathbf{A}^2 \\ \mathbf{A}^3 \\ \vdots \\ \mathbf{A}^N \end{bmatrix}, \mathbf{G} = \begin{bmatrix} \mathbf{B} & 0 & \dots & 0 \\ \mathbf{A}\mathbf{B} & \mathbf{B} & \dots & \vdots \\ \vdots & \vdots & \ddots & \vdots \\ \mathbf{A}^{H_N-1}\mathbf{B} & \mathbf{A}^{H_N-2}\mathbf{B} & \dots & \mathbf{B} \end{bmatrix}. \quad (18)$$

Using this formulation, the horizon output predictions take the form:

$$\mathbf{z}(k) = \mathbf{C}[\mathbf{F}\mathbf{x}(k) + \mathbf{G}\mathbf{u}_{ss}]. \quad (19)$$

We assume that at a given reference point $\mathbf{r}(k)$, exists a steady state \mathbf{x}_{ss} with a steady-state input \mathbf{u}_{ss} . It is then possible to use the system dynamics to define the input required to maintain the reference (20)

$$\begin{bmatrix} \mathbf{I}_{12 \times 12} - \mathbf{A} & -\mathbf{B} \\ \mathbf{C} & \mathbf{D} \end{bmatrix} \begin{bmatrix} \mathbf{x}(k)_{ss} \\ \mathbf{u}(k)_{ss} \end{bmatrix} = \begin{bmatrix} \mathbf{0}_{12 \times 1} \\ \mathbf{r}(k) \end{bmatrix}. \quad (20)$$

Solving equation (20) for a given reference output $\mathbf{r}(k)$ allows the steady state $\mathbf{x}(k)_{ss}$ and input $\mathbf{u}(k)_{ss}$ to be determined. Calculation of this value allows the absolute input to be defined as a difference between the reference control and the control signal generated by the controller.

The predicted error over the horizon is defined by:

$$\mathbf{e}(k) = \mathbf{r}(k) - \mathbf{z}(k). \quad (21)$$

Here, the error is that between the reference signal and the system output over the prediction horizon H_N . The tracking error and control weightings over the horizon are also defined as the following:

$$\mathbf{Q}_{H_p} = \begin{bmatrix} \mathbf{Q} & 0 & \dots & 0 \\ 0 & \mathbf{Q} & \dots & \vdots \\ \vdots & \vdots & \ddots & \vdots \\ 0 & \dots & \dots & \mathbf{N} \end{bmatrix}, \mathbf{R}_{H_p} = \begin{bmatrix} \mathbf{R} & 0 & \dots & 0 \\ 0 & \mathbf{R} & \dots & \vdots \\ \vdots & \vdots & \ddots & \vdots \\ 0 & \dots & \dots & \mathbf{R} \end{bmatrix}, \quad (22)$$

where \mathbf{Q} , \mathbf{R} and \mathbf{N} are weighting matrices.

The cost function can then be derived to evaluate the optimal control inputs as a function of the predicted error, control effort $\mathbf{u}(k)$ and a terminal error at the horizon (23)[11],[14]:

$$V(k) = \sum [\|\mathbf{r}(k) - \mathbf{z}(k)\|^2 \mathbf{Q} + \|\mathbf{u}(k)\|^2 \mathbf{R}] + \|\mathbf{r}(k) - \mathbf{z}(k)\|^2 \mathbf{N}. \quad (23)$$

Here $\|u(k)\|$ is used to describe the Euclidean norm of the input. Substituting the horizon prediction matrix expressions allows equation (23) to be redefined as quadratic coefficients of the control input $\mathbf{u}(k)$. The terminal cost matrix \mathbf{N} can be seen neglected, with no value assigned to a terminal angular rate:

$$V(k) = \mathbf{u}(k)^T [\boldsymbol{\Theta}^T \mathbf{Q} \boldsymbol{\Theta} + \mathbf{R}] \mathbf{u}(k) - 2\mathbf{u}(k)^T \boldsymbol{\Theta}^T \mathbf{Q} \mathbf{e}(k) + \mathbf{e}(k)^T \mathbf{Q} \mathbf{e}(k), \quad (24)$$

where:

$$\boldsymbol{\Theta} = \mathbf{C} \mathbf{G}. \quad (25)$$

If $\mathbf{H} = \boldsymbol{\Theta}^T \mathbf{Q} \boldsymbol{\Theta} + \mathbf{R}$ and $\mathbf{G} = -2\boldsymbol{\Theta}^T \mathbf{Q} \mathbf{e}(k)$ then the cost function takes the reduced form [14]:

$$V(k) = \mathbf{u}(k)^T \mathbf{H} \mathbf{u}(k) + \mathbf{u}(k)^T \mathbf{G} + \mathbf{e}(k)^T \mathbf{Q} \mathbf{e}(k). \quad (26)$$

The optimal control sequence then occurs where equation (26) is minimal, subject to the dynamics of the system and design constraints. This optimisation operation was computed directly using the Matlab function *quadprog*. The first of the optimal control inputs is then used to instigate a change in the system state (16).

A series of design constraints are also introduced to represent the performance limits of the quadrotor aircraft:

$$-35^\circ \leq \phi, \theta \leq 35^\circ, \quad (27a)$$

$$0 \text{ rad/s} \leq \Omega_{1-4} \leq 580 \text{ rad/s}. \quad (27b)$$

A regime was then applied to define a set of maximum deflection angles to prevent inversion and to aid in maintaining stability (27a). The above input conditions (27b) were then selected to represent the physical limits of the actuators on board the F450 quadrotor.

Initially, the state and input weighting matrices \mathbf{Q} and \mathbf{R} of the LQR controller were used as a benchmark value in tuning the MPC characteristics. A step response was then used to observe the performance over different prediction horizons.

4.2 Linear Quadratic Regulation (LQR)

The Linear Quadratic Regulator (LQR) controller acts to resolve the optimum feedback gain \mathbf{K} which symbolises the control effort and the transient response of the system. The optimal solution is found by evaluating the minimum value of a cost function J_{QR} ; containing weightings of the plant (\mathbf{Q}) and the control inputs (\mathbf{R}). The cost function is then of the form:

$$J_{QR} = \min \int [\mathbf{x}(t)^T \mathbf{Q} \mathbf{x}(t) + \mathbf{u}(t)^T \mathbf{R} \mathbf{u}(t)] dt. \quad (28)$$

Here the input vector $\mathbf{u}(t)$ represents the rotor speeds applied to the system as a result of the control mapping, derived from inverting the expression in equation (13) or directly. The result of optimal control problem is then a state feedback gain ($\mathbf{u} = -\mathbf{K}\mathbf{x}$) where J_{QR} is minimal, subject to the dynamics $\dot{\mathbf{x}} = \mathbf{A}\mathbf{x} + \mathbf{B}\mathbf{u}$. The system input is then the sum of the state feedback and a reference set point $\mathbf{r}(t)$:

$$\mathbf{u}(t) = \mathbf{r}(t) - \mathbf{K}\mathbf{x}(t). \quad (29)$$

Here the matrix \mathbf{K} is the solution to the algebraic Riccati equation

$$\mathbf{A}^T \mathbf{P} + \mathbf{P} \mathbf{A} - \mathbf{P} \mathbf{B} \mathbf{R}^{-1} \mathbf{B}^T \mathbf{P} + \mathbf{Q} = 0, \quad (30)$$

where the feedback is defined as:

$$\mathbf{K} = \mathbf{R}^{-1} \mathbf{B}^T \mathbf{P}. \quad (31)$$

The LQR feedback gain is then used to instigate state feedback in the aircraft's dynamic expressions (16).

5 Performance Evaluation

The designed MPC algorithm is evaluated by observing the systems transient response to a step input. The results are then directly compared to the response of the LQR, subject to the same inputs. Both controllers are designed to obtain a reference roll, pitch and yaw rate $\dot{\phi}, \dot{\theta}, \dot{\psi}$, respectively, as preliminary attitude controllers for the VTOL aircraft.

The gain matrices \mathbf{Q} and \mathbf{R} are to be selected to instigate the desired transient responses in each axis. The LQR gain matrices \mathbf{Q} and \mathbf{R} are initially defined by identity matrices of the form $\mathbf{Q} = \mathbf{C}^T \mathbf{C}$ and $\mathbf{R} = \mathbf{I}_{4 \times 4}$. Each LQR gain was then tuned heuristically until a critically damped step response, with an amplitude of 0.5rad/s was observed. The relative settling times, overshoot and sensitivity to noise could then be compared, on Figure 4.

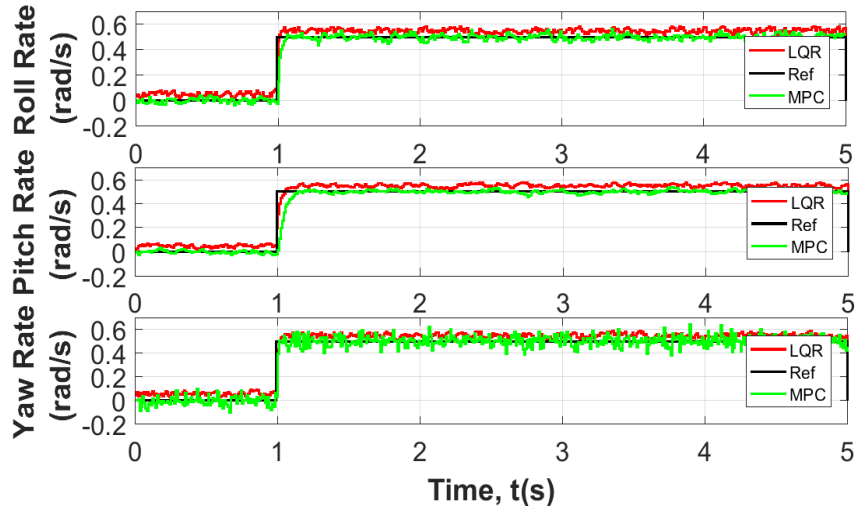


Fig. 4: The aircraft’s response to a step input of 0.5rad/s under the MPC and LQR control regimes.

The MPC gain matrices are initially set to be the resultant LQR gains. The prediction horizon is then varied to optimise the response to a step input.

The responses of the two control regimes (LQR and MPC) controllers shown in figure 4. Both controllers can be seen to stabilise the system about a reference axis rate (Ref) of 0.5rad/s. Some steady-state error can be seen in the LQR output as a result of the Gaussian noise added to the system. This is likely due to the deviation away from the linear system and some integral feedback is required. The response of the MPC controller can then also be seen to achieve the desired rates in equivalent conditions. The mean settling times of the two controllers were then calculated based on one hundred Monte-Carlo experiments (see Table 1).

Table 1: A comparison of the LQR/MPC mean settling times, in seconds, following one hundred Monte-Carlo iterations.

Controller	Roll Rate $t_{set}(s)$	Pitch Rate $t_{set}(s)$	Yaw Rate $t_{set}(s)$
LQR	0.10	0.22	0.11
MPC	0.09	0.20	0.05

As seen in Table 1, the LQR and MPC algorithms demonstrate similar performance in the presence of the Gaussian noise signal. The MPC controller is however shown to be able to settle the system faster, with no overshoot or steady

state error. The constraints applied with in the MPC demonstrated further tolerance to noise through minimal steady-state error. The optimal inputs of the MPC are also found considering the physical limits of system which the LQR cannot do directly. This allows the algorithm to plan the inputs around the possibility of the VTOL system reaching actuator saturation or a limit on the physical output.

6 Conclusions

In this paper, a symbolic approach to modelling Vertical Takeoff and Landing (VTOL) vehicles was presented. The dynamics and numeric definition of a small quadrotor UAV are also introduced as a basis for the design of both a Linear Quadratic Regulator and Model Predictive attitude controllers. Both controllers were successful in stabilising the aircraft about a given reference rate of 0.5rad/s in the presence of white noise signal. A comparison of the controllers demonstrated that the MPC was able to achieve the desired state quicker than the LQR on average, but also demonstrated minimal steady-state error and overshoot.

The proposed approach has the potential in a number of applications, especially in adaptive control algorithms for complex UAV topologies. Derivation of both the linear and non-linear systems in such cases facilitate their stability analysis. Future work in this area will focus be on the derivation of non-linear control strategies on non-linear representations of other UAV systems. Scope also exists for the symbolic calculation of the Lyapunov functions and their application to further VTOL systems.

References

1. D. Ho A. Grancharova, E.I. Grtli and T.A. Johansen. Uavs trajectory planning by distributed mpc under radio communication path loss constraints. *Journal of Intelligent & Robotic Systems*, 79(1):115–134, 2014.
2. S. Bouabdallah and R. Siegwart. Full control of a quadrotor. In *Intelligent robots and systems, 2007. IROS 2007. IEEE/RSJ international conference on*, pages 153–158. IEEE, 2007.
3. P. Bouffard. On-board model predictive control of a quadrotor helicopter: Design, implementation, and experiments. Technical report, DTIC Document, 2012.
4. Z. Chao, S.-L. Zhou, L. Ming, and W.-G. Zhang. UAV Formation Flight Based on Nonlinear Model Predictive Control. *Mathematical Problems in Engineering*, 2012(261367):15, 2012.
5. D. Diehl, H. Ferreau, and N. Haverbeke. *Nonlinear Model Predictive Control: Towards New Challenging Applications*, chapter Efficient Numerical Methods for Nonlinear MPC and Moving Horizon Estimation, pages 391–417. Springer Berlin Heidelberg, Berlin, Heidelberg, 2009.
6. ESDU. Quaternion representation of aeroplane attitude. Technical report, The Royal Aeronautical Society, 2002.
7. ESDU. Introduction to aerodynamic derivatives, equations of motion and stability. Technical Report 86021c, The Royal Aeronautical Society, 2003.

8. T. I. Fossen. Mathematical models for control of aircraft and satellites. *Department of Engineering Cybernetics Norwegian University of Science and Technology*, 2011.
9. G. Frison, H. H. B. Srensen, B. Dammann, and J. B. Jrgensen. High-performance small-scale solvers for linear model predictive control. In *Control Conference (ECC), 2014 European*, pages 128–133, June 2014.
10. T.I. Johansen. Toward Dependable Embedded Model Predictive Control. *Systems Journal, IEEE*, PP(99):1–12, 2014.
11. K. Kunz, S. M. Huck, T. H. Summers, and J. Lygeros. Fast model predictive control of miniature helicopters. In *Proc. of the IEEE European Control Conference*, pages 1377 – 1382, 2013.
12. B. Landry, R. Deits, P. Florence, and R. Tedrake. Aggressive quadrotor flight through cluttered environments using mixed integer programming. 2015.
13. C. Liu, W.-H. Chen, and J. Andrews. Explicit non-linear model predictive control for autonomous helicopters. *Proceedings of the Institution of Mechanical Engineers, Part G: Journal of Aerospace Engineering*, 226:1171–1182, 2011.
14. J.M. Maciejowski. *Predictive Control with Constraints*. Pearson Education, Harlow, England, 1 edition, 2002.
15. M. Moness and M. Bakr. Development and Analysis of Linear Model Representations of the Quad-Rotor System. *Proceedings from the 16th International Conference on Aerospace Sciences & Aviation Technology*, 2015.

Acknowledgement: The authors gratefully acknowledge the support from the UK EPSRC under grant number EP/M506618/1.